Intelligent Transportation and Smart Cities
V. Mezhuyev et al. (Eds.)

doi:10.3233/ATDE240373

Research on Anti-Skid-Rotation Control Strategy of Dual-Motor Four-Wheel-Drive Electric Vehicle Drive

Tian ZHANG[1]
Department of Mechanical and Electrical Engineering, Heilongjiang Institute of Construction Technology, Harbin, China

Abstract. This paper focuses on the research of longitudinal and lateral instability of dual motor electric vehicles during driving. The main objective is to ensure that the vehicle maintains both longitudinal and lateral stability during acceleration and steering, and also to ensure dynamic performance. The study involves the design of a drive anti-skid steering control system and a handling stability control system, with coordination between the two. To achieve this, the study analyses the vehicle's different performance and stability requirements at different speeds. It sets a speed threshold where performance is prioritized at low speeds and stability is prioritized at high speeds. Based on these requirements, the activation conditions of the control system are designed for different speed ranges. Results from simulation verification under two different operating conditions - acceleration and steering - show that the control systems can effectively manage wheel slip rates to stay within 0.02 of the optimum slip rate for the road surface when the wheels slip. In addition, the deviation of the actual yaw rate from the setpoint is kept below 16% of the setpoint when the vehicle is experiencing lateral instability. The control strategy developed not only improves the stability and dynamics of the dual-motor electric vehicle but also has academic implications for improving vehicle stability and dynamics in general.

Keywords. Dual-motor electric vehicle, drive slip, handling stability, torque distribution, braking torque distribution

1.Introduction

This paper examines the importance of designing a safe and reliable drive structure for electric vehicles, particularly in cases where electronic components may fail during operation. The traditional drive structure of electric vehicles is no longer sufficient to meet safety requirements, as evidenced by incidents involving single-motor electric vehicles experiencing sudden failure. To address these concerns, this study focuses on electric vehicles with independent front and rear axles, which have several advantages over conventional electric vehicles. These vehicles do not require a fixed ratio of motor torque distribution, allowing greater flexibility in control strategies. With two motors at the front and rear axle, independent control of the wheel torque distribution can be achieved, allowing optimized torque distribution for improved vehicle stability and safety performance. Vehicle stability is maintained by adjusting the torque distribution,

[1] Corresponding Author: Tian ZHANG, 14508128@qq.com.

helping to prevent sudden stops and potential accidents. In addition, the all-wheel drive mode provides increased power to the vehicle, improving its overall performance compared to conventional front- or rear-wheel drive electric vehicles. In conclusion, this paper emphasizes the need for innovative drive structures in electric vehicles to ensure safety and performance during operation. The use of front and rear independent drive systems offers a promising solution to improve vehicle stability and safety while increasing overall performance.

The objective of this thesis is to develop an advanced anti-skid steering control strategy for dual-motor electric vehicles that address the limitations of traditional PID control in adapting to varying road conditions. The research explores the integration of fuzzy control and neural network techniques to enhance the adaptive capabilities of the PID controller and improve its performance in optimal slip rate control.[1]The proposed control strategy involves a two-level approach: the upper level applies optimal slip rate control to the front and rear wheels to determine the total torque required for the front and rear axles, while the lower level calculates the torque distribution based on the speed differences between the front and rear axles.[2,3]This hierarchical structure ensures that torque is effectively distributed throughout the car's driveline. A key innovation in this study is the consideration of engine torque transfer during slip events, allowing more efficient use of available torque. The control strategy prioritizes torque redistribution when wheel slip occurs, maximizing traction and stability. Overall, this paper presents a comprehensive solution for improving the anti-skid steering control of dual-motor electric vehicles by combining traditional PID control with advanced fuzzy and neural network techniques. The proposed control strategy provides improved adaptability to different road conditions and optimizes torque utilization, contributing to the advancement of electric vehicle technology and safety.

2.Methodology Research Basis

When a dual-motor four-wheel drive electric vehicle is under drive anti-skid control, the two motors of the front and rear axles drive the left and right wheels of the front and rear axles independently, which is different from that of a hub-motor electric vehicle that can realize the control of a single wheel, so this paper designs the drive anti-skid control strategy for a dual-motor four-wheel drive electric vehicle. A control strategy based on the radial basis function PID adaptive control algorithm is designed to realize the drive anti-skid for dual-motor four-wheel drive electric vehicles. The system structure of the dual-motor four-wheel drive electric vehicle and the working principle of the drive anti-skid steering control were analyzed, and the simulation analysis was carried out on different road surfaces by monitoring the slip rate of the vehicle during driving and the optimal slip rate of the current road surface, and controlling the torque distribution of the front and rear motors through the control system. The results show that the control strategy can achieve anti-skid-rotation control under different working conditions.

2.1. Road Recognition

- Relationship between slip rate and adhesion coefficient

The dynamics of the car is limited by the attachment conditions so that there exists a maximum value of the tangential force of the car, which is often defined as the attachment force as in the following equation (1):

$$F_{x\max} = \mu F_z \tag{1}$$

To prevent the vehicle from slipping while driving, it is necessary to control the ground tangential reaction force generated by the driving torque provided to the wheels by the engine torque so that it is less than the adhesion force as shown in the following equation (2):

$$F_x \le \mu F_z \tag{2}$$

Wheel slip occurs when the adhesion of the road surface is exceeded, usually defined as the slip rate according to the following equation (3):

$$s = \frac{V_{\mathbf{round}} - V_x}{V_{\mathbf{round}}} \tag{3}$$

The adhesion force is directly related to the road surface adhesion coefficient and the vertical load and is greatly affected by the road surface adhesion conditions when the vertical load does not change.

If the optimum slip rate is set at a fixed value, when the road surface on which the vehicle is traveling changes, the control will be adversely affected by the change in the optimum slip rate. Therefore, in anti-skid steering control, road surface identification of the current road surface is an important part of the control.

- Tyre and road mode

In addition to selecting a fixed target value, there are two methods of determining the optimum slip rate by identifying the shape and parameters of the curve when performing the drive skid control. The method of identifying the optimum slip rate based on the shape of the curve is to identify the optimum slip rate of the current road surface based on the slope of the curve when the slip rate is low. This method has some limitations and cannot adapt to the change in slip rate in different situations.[4,5] Due to the limitations of the first two methods, this paper uses the method based on curve parameter identification to identify the optimum slip rate of the pavement. The curve parameter identification method is mainly based on the tire model to determine the road adhesion coefficient and the optimum slip rate, and the commonly used tire and road surface models are the Burckhardt model, the Kiencke model, the "magic formula" model, and so on. Of the three models, the Burckhardt model uses only three fitting parameters that can represent the characteristics of the model with high accuracy. The Burckhardt, the relationship between the road adhesion coefficient and slip rate for the model is as shown in the following equation (4):

$$\mu(s) = C_1(1 - e^{-C_2 s}) - C_3 s \tag{4}$$

$C_1, C_2 and C_3$ are the fitting coefficient for the pavement.

After determining the three fitting parameters C_1, C_2, and C_3, the peak adhesion coefficient and the optimum slip rate of the road surface on which the wheel is located can be estimated from the following equation. The peak adhesion coefficient and the optimum slip rate of the wheel can be estimated according to the following equation as shown in the following equations (5) and (6).

$$S_{opti} = \frac{1}{C_2} \ln \frac{C_1 C_2}{C_3} \tag{5}$$

$$\mu_{\max i} = C_1 - \frac{C_3}{C_2}(1 + \ln \frac{C_1 C_2}{C_3}) \tag{6}$$

2.2. Radial Basis Function PID Adaptive Control Algorithm

Neural networks, with their exceptional non-linear mapping capabilities, precise ability to approximate non-linear functions, and fast convergence features, can operate effectively in complex environments. The neural network PID controller is a powerful combination of neural networks and PID controllers that effectively compensate for the shortcomings of traditional PID in terms of anti-interference capability and adaptability. In short, the neural network PID controller is like adding wings to a tiger, making control more precise and efficient.[6,7]

In the schematic (Fig. 1), the controller's two inputs are the instantaneous slip rate and the deviation from the optimum slip rate for the current road conditions. The output is a torque adjustment value calculated by the PID controller. This adjusted torque value from the previous (k-1) moment is then fed into the control object system, resulting in a post-control slip rate. Simultaneously, the radial basis function neural network processes the torque adjustment amount, the post-control slip rate, and the slip rate after adjustment at the (k-1) moment. It provides Jacobian information for PID parameter tuning. The refinement algorithm is articulated in equation (7), which is not shown here but is central to the optimization process.[8-10]

$$\begin{cases} \Delta k_P = \eta_P e(k) \dfrac{\partial y}{\partial \Delta u} x_c(1) \\ \Delta k_I = \eta_I e(k) \dfrac{\partial y}{\partial \Delta u} x_c(2) \\ \Delta k_D = \eta_D e(k) \dfrac{\partial y}{\partial \Delta u} x_c(3) \end{cases} \tag{7}$$

Where Δk_P , Δk_I , and Δk_D are the adjustments of the parameters k_P , k_I ,and k_D respectively. η_P , η_I and η_D are the adjusted rates for Δk_P , Δk_I ,and Δk_D .The Jacobian information used in equation (7) and the learning algorithm of each parameter of the recognition network are the parameter formulas in the above RBF neural network algorithm.

2.3. Design of Drive Anti-skid Rotation Control Strategy

The logic of the traction control system is shown in Figure 2. According to the real-time monitoring of the vehicle information and the current road adhesion, the optimum slip rate S opt is determined. Since the purpose of the slip rate control is to control the slip rate close to the optimum slip rate, if the real-time slip rate exceeds the optimum slip rate by 0.02, the drive anti-slip control is activated.

2.4. Validation of Drive Anti-skid Rotation Control Strategy

Set the vehicle to drive from the high-adhesion surface to the low-adhesion surface, set the high-adhesion coefficient to 0.6, the low-adhesion coefficient to 0.19, the initial speed to 10m/s, and the wheel turning angle to 0°fixed.[11]Select two wheels on the same side for observation. The simulation results of the slip rate, motor torque, and vehicle speed before and after the control are shown in Figure 3.

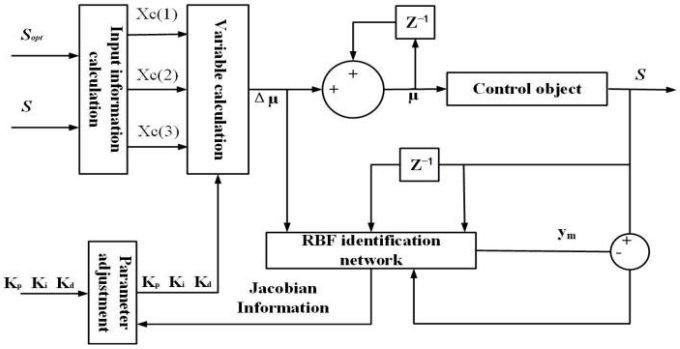

Figure 1. Radial basis function PID controller.

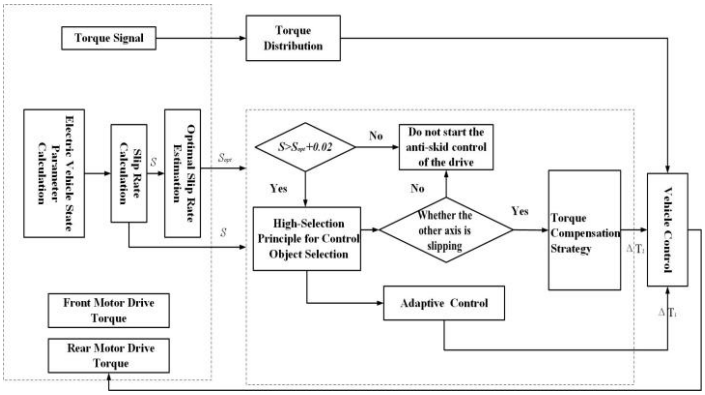

Figure 2. Drive anti-skid control strategy.

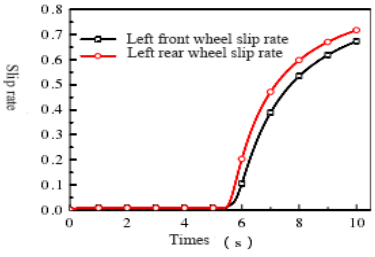

(a) Left-hand wheel slip rate when uncontrolled

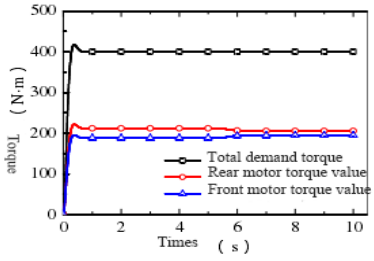

(b) Motor torque distribution without control

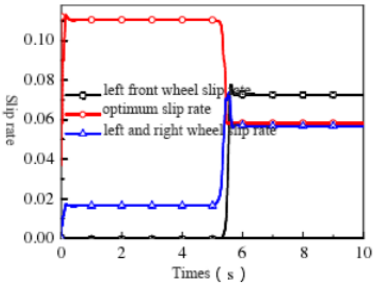

(c) Control of rear left-hand wheel slip rate

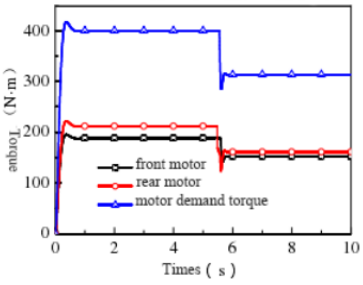

(d) Control of rear motor torque distribution

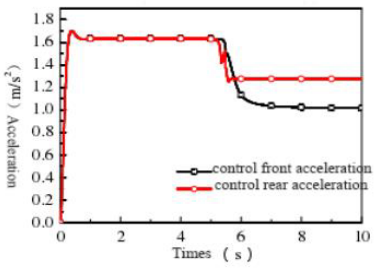

(e) Comparison of acceleration

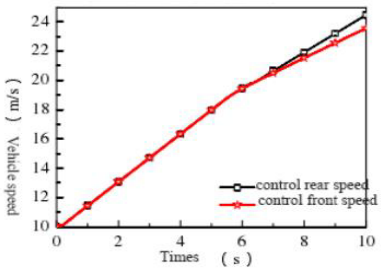

(f) Speed comparison before and d after control

Figure 3. Simulation results of docking pavement.

According to Figure 3(a), when the vehicle is driving on a high-adhesion surface, the wheels do not exhibit any slipping. However, once the vehicle enters a low adhesion surface, it begins to skid and quickly spreads in a short period. By observing the torque change charts before and after control in Figure 3(b, d), it can be found that once the vehicle enters the low adhesion surface, merely adjusting the torque distribution of the front and rear motors is not sufficient to effectively control the wheel slip rate. The left rear wheel has a higher slip rate, hence the traction slip control of the rear axle motor is activated, along with the torque compensation control strategy for the front axle motor. Through the implementation of traction slip control and torque compensation strategies, the rear wheel's slip rate is controlled as shown in Figure 3(c), bringing the slip rates of both the front and rear axle wheels close to the optimal slip rate. Comparing Figure 3(a, b), it can be seen that without skidding, the anti-skid control will not be activated; but when the wheels begin to skid, the anti-skid control can immediately execute control on the motors of the skidding axle. Ultimately, the slip rate of the left rear wheel is controlled at 0.056, and the slip rate of the left front wheel is controlled at 0.072, both within the set stability range of 0.02. Figure 3(e, f) shows the situation where the left rear wheel's slip rate is controlled at 0.056. From Figure 3(e, f), it can be observed that without skidding, the acceleration and speed remain constant; but after the wheels skid and are controlled, at the end of the simulation, the acceleration and speed reached 1.27m/s² and 24.5m/s respectively, which are higher than the pre-control values of 1m/s² and 23.5m/s. Therefore, on composite road surfaces, the applied control ensures the longitudinal stability of the whole vehicle and enhances its longitudinal dynamic performance, verifying the effectiveness of the designed anti-skid steering control strategy.

3. Research Methods

The dual-motor four-wheel drive electric vehicle ensures that the left and right wheels, controlled by the front and rear motors, have the same drive force through a differential mechanism. It is not possible to control individual wheels for stability control, but the wheels can be hydraulically controlled separately. According to the control algorithm, the amount of additional swing torque is determined by the hydraulic simulation model based on the rules of each variable to determine which wheels need to apply braking torque and finally achieve swing torque control.

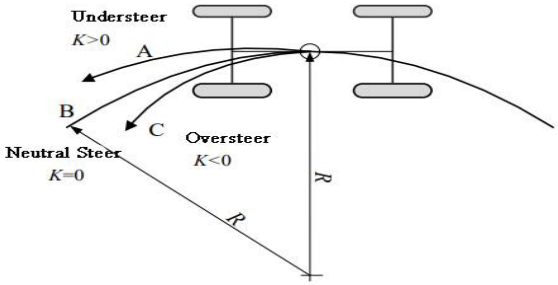

Figure 4. Vehicle steady-state response diagram.

3.1. Vehicle Instability Analysis

At present, serious traffic accidents are mainly caused by the lateral instability of vehicles traveling on low-adhesion surfaces or at high speeds, and the driver is unable to make an active response. Transverse pendulum motion due to the generation of front wheel angle, the car began to curve motion, affected by the centrifugal force so that the wheels produce lateral force so that the front wheels produce lateral deflection angle. The occurrence of transverse pendulum motion causes the rear wheels to generate a lateral turning angle, so the rear wheels generate a lateral force due to the generation of the lateral turning angle.[12,13] The attachment ellipse relationship that exists between the lateral and longitudinal tire forces will result in lateral instability when the tire forces exceed the attachment ellipse. Stability is the ability of a vehicle to follow the driver's intended direction of travel when the driver is not fatigued and to remain stable when subjected to external disturbances. A vehicle's handling stability is often characterized by the vehicle's steady-state steering behavior, as shown in Figure 4.

Control of handling stability is divided into two parts: trajectory capability, characterized by the side-slip angle of the center of gravity; and stability, characterized by the roll angular velocity, determined by the vehicle's roll torque. The purpose of controlling vehicle stability is to suppress understeer or oversteer. As shown in Figure 5, the C curve indicates that if the vehicle tends to oversteer, this means that a small steering angle can produce a large swing angular velocity. At this time, the steering radius is also smaller than the radius of neutral steering, which makes it prone to skidding or rolling over, posing a risk of losing stability. Therefore, cars should have a sufficient understanding of characteristics.

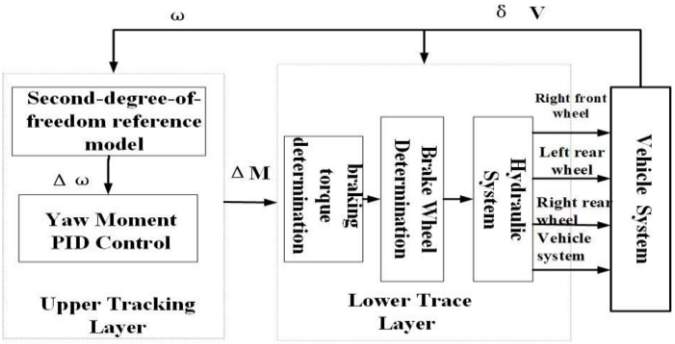

Figure 5. Control logic diagram of handling stability.

3.2. Design of Vehicle Maneuvering Stability Control Strategy

The lateral swing angular velocity to a certain extent reflects the stability of the vehicle and can be controlled by the direct lateral swing torque control method through the lateral swing angular velocity, so the control of the lateral swing angular velocity also achieves the control of the vehicle's lateral driving stability. For the lateral swing stability control of dual-motor four-wheel drive electric vehicles, this paper adopts a hierarchical control based on the principle of lateral swing stability control of dual-motor four-wheel drive electric vehicles, as shown in Figure 5.

The upper layer tracking controller collects driver information and calculates the current additional vehicle yaw moment and vehicle dynamic requirements based on the two-degree-of-freedom vehicle reference model, wheel angle, and current vehicle feedback information. This information is then transmitted to the lower braking torque distribution layer. The lower layer is the braking torque distribution layer, which obtains the additional lateral torque through the control algorithm. This torque is converted into braking torque applied to the wheels via the hydraulic system. Then, based on the wheel angle and lateral angular velocity deviation, it determines which wheel to apply the braking force to, thereby achieving control of the vehicle's lateral stability.

3.3. Top Layer Design for Vehicle Maneuverability and Stability

- Control value determination

The driving stability of a car has two aspects: Firstly, the car must be able to drive according to the driver's intention and ensure that the driving path does not deviate; secondly, the stability of the lateral oscillation during driving so that the vehicle does not produce dangerous phenomena such as side-slip during driving. The first problem is usually represented by the center of gravity lateral deviation angle and the second by the yaw angular velocity. When the vehicle is in an extremely unstable state, stability is usually expressed by the center of gravity slip and yaw angular velocity. When the vehicle is in a stable linear region, the driver's intention can be fully expressed by the yaw angular velocity. Therefore, by controlling the yaw angular velocity, the lateral stability of the vehicle can be reflected, and the lateral stability of the vehicle can be achieved by controlling the yaw torque. This paper mainly studies the maneuverability of vehicles in stable linear regions, so the yaw angular velocity is used as the control variable for the yaw torque control.[14,15]

To control the vehicle to have appropriate understeer characteristics, it is first necessary to determine what type of steady-state response the vehicle motion is. In this paper, lateral moment control is performed using lateral angular velocity as the control variable, and the steady-state response of the vehicle can be judged using the lateral angular velocity and other inputs as criteria. When judging the steady-state response of the vehicle, a fixed steering angle is input into the stationary vehicle, causing the vehicle to perform a circular motion at different speeds to obtain the absolute values of the lateral slip angles of the front and rear wheels. The difference between the two is used as a criterion for judging the steady-state response of the vehicle, as shown in equation (8):

$$\alpha_1-\alpha_2=\begin{cases}>0,\text{Understeer}\\=0,\text{Neutral Steer}\\<0,\text{Oversteer}\end{cases} \tag{8}$$

The following relationship exists between the angular velocity of the horizontal pendulum and the difference in side deflection angles of the front and rear wheels, as shown in equation (9):

$$\alpha_1-\alpha_2=\frac{l\gamma-\delta v}{v} \tag{9}$$

Therefore the relationship between the transverse pendulum angular velocity and the steady state response of the car can be obtained from Eq. 8 and Eq. 9:

$$\alpha_1-\alpha_2=\begin{cases}>\dfrac{\delta v}{l},\text{Understeer}\\=\dfrac{\delta v}{l},\text{Neutral Steer}\\<\dfrac{\delta v}{l},\text{Oversteer}\end{cases} \tag{10}$$

If the centroid side slip angle is not considered or is relatively small, the vehicle's steady-state response can be assessed by the swing angular velocity, wheel slip angle, and vehicle speed, which can further determine whether the vehicle is unstable. It can also be seen from equation (10) that controlling the swing angular velocity can improve handling stability.

- Tracking Controller

From equation 9 it can be seen that when a steering angle is applied to control the vehicle, the lateral angular velocity of the vehicle is linearly related to the turning angle. At this point, the response of the vehicle can be used as an ideal reference for control. When the tires are in a non-linear range during driving, the response of the vehicle to turning is the actual value which has a certain deviation from the control reference value. To control the lateral angular velocity, it is necessary to establish a vehicle model that reflects the linear relationship between the lateral angular velocity and the turning to obtain the reference value of the lateral angular velocity.

The motion control tracker is based on a reference model and control variables. The reference model assumes the steering angle of the wheels and then calculates the reference values of the control variables based on the current state of the vehicle. In this paper, a two-degree-of-freedom vehicle model is used as the reference model because it eliminates the influence of the suspension; the vehicle does not experience lateral motion, vertical motion, or air resistance. The derived lateral angular velocity is therefore more accurate than the required control variable value. As mechanical systems generally exhibit lags, it is important to avoid system instability caused by large overshoots in the lateral angular velocity response. To this end, we simplify the dynamic response process of lateral angular velocity and front wheel angle by introducing a first-order delay element. The result is a primary system and equation (11) describes the expected lateral angular velocity.

$$\gamma_d=\frac{u}{l(1+kV_x^2)}\times\frac{1}{\tau_r s+1}\delta \tag{11}$$

where δ is the front wheel angle, V_x is the vehicle speed, k represents the stability factor, τ_r is the time constant and l is the wheelbase. The stability factor k is calculated as in the following equation (12):

$$k = \frac{m}{l^2}\left(\frac{a}{k_2} - \frac{b}{k_1}\right) \tag{12}$$

During the driving process, the adhesion conditions between the tires and the road surface have a significant effect on safe driving. For this reason, direct yaw control must take into account the road adhesion conditions, making sure that the yaw angular velocity setpoint doesn't exceed the maximum yaw angular velocity of the current road surface.A vehicle's ideal sideways speed can be calculated from its road adhesion and overall system constraints on sideways speed stability, according to (13):

$$\gamma^* = \min\left\{|\gamma_d|, \left|\frac{\mu g}{V_x}\right|\right\} \cdot \mathrm{sgn}(\delta) \tag{13}$$

- Motion tracking layer control algorithm

Define the deviation of the reference value of the traverse angular velocity obtained by the two-degree-of-freedom reference model from the actual traverse angular velocity of the vehicle to judge the stability of the vehicle. If the absolute value of the deviation of the angular velocity of travel exceeds the specified limits, the system will become unstable. According to equation 14, this range is used as a criterion to determine the effectiveness of the control strategy when assessing the stability of the vehicle:

$$|\Delta\gamma| = |\gamma - \gamma^*| \le |C \cdot \gamma^*| \tag{14}$$

In the above equation: C = 0.16

The deviation $\Delta\gamma$ between the reference swing angle velocity and the actual swing angle velocity is used to determine whether Eq.14 is satisfied as a stability judgement.

With the actual control, to minimize understeering, the maneuvering stability control is activated when the absolute value of the peak of the actual angular velocity is greater than the peak of the reference value. After the swing torque control system is activated, the swing angular velocity deviation is used as the input to the controller, and the additional swing torque is input to the lower braking force distribution layer through PID control.

3.4. Brake Force Distribution Layer

Under certain working conditions, it is necessary to obtain additional swing moment, but this additional swing moment cannot be directly applied to the vehicle itself. It is usually through a system that the additional swing moment is applied to the wheels, thus achieving stability control. In this paper, the controlled vehicle model is an electric car with dual-motor four-wheel drive, featuring independent front and rear axle drives. The characteristics of the front and rear axle motors control the wheels on both sides, making it impossible to change the lateral torque by controlling the motor drive torque. However, this can be achieved by hydraulically controlling the wheels. By applying hydraulic braking torque to different wheels under different working conditions according to the additional swinging moment obtained from the upper control tracking layer, the swinging angular velocity can be controlled.

- Hydraulic system simulation model

The modelling of the hydraulic system needs to involve the interaction between machinery and hydraulics, and detailed parameters of each component are required for simulation. In this article, only a transfer function reflecting the dynamic characteristics of the hydraulic system is required to verify the accuracy of the control strategy,

without considering the effect of the hydraulic system components on the overall hydraulic system. Therefore, the following simplified first-order equivalent model is used as shown in equation (15):

$$G_h(s) = \frac{e^{-T_{hd} \cdot S}}{1 + T_h \cdot s} \tag{15}$$

In the above equation: T_h is the time constant of inertial link, take the value of 0.208; T_{hd} is the output delay time, take the value of 0.124.

- Hydraulic brake force distribution

The additional yaw torque generated by the upper-level tracker control is distributed using a hydraulic differential braking method. The steady-state behavior of the vehicle is determined from parameters fed back during the driving process. The principle of hydraulic differential braking is to select the most appropriate wheel to apply the braking force. The additional yaw moment calculated at the higher level is converted into the hydraulic braking force applied to the wheels, thus controlling the yaw rate. Control to maintain the stability of vehicle steering. According to the vehicle steering steady state response analysed in the previous section, the vehicle instability conditions are classified into four types: understeer and oversteer when turning left and right.

If oversteering occurs during a left turn, the rear axle tires enter a non-linear region and the lateral angular velocity exceeds the reference value. An additional clockwise lateral torque is required, so hydraulic braking must be applied to the right front wheel. Conversely, if understeering occurs during a left turn, the front axle tires enter a non-linear region and the lateral angular velocity falls below the reference value. An additional anti-clockwise lateral torque is required, so hydraulic braking should be applied to the left rear wheel. In the case of the right oversteer, the rear axle tires are in a non-linear area and the lateral angular velocity is greater than the reference value. To correct the excessive clockwise lateral torque, hydraulic braking must be applied to the left front wheel. The last unstable scenario is understeering to the right, where the front tire of the front axle enters a non-linear region and the lateral angular velocity is less than the reference value. To correct the insufficient counterclockwise lateral torque, hydraulic braking should be applied to the right rear wheel. When the vehicle rotation angle is zero, there may still be a lateral angular velocity deviation due to certain factors. At this point, the reference value for lateral angular velocity is zero. Regardless of the direction or magnitude of the lateral angular velocity deviation, the result is oversteering. If the deviation value is greater than zero, it is similar to oversteering during a left turn; if the deviation value is less than zero, it is similar to oversteering during a right turn.

- Hydraulic braking force determination

When distributing the additional swing torque for hydraulic differential braking, it is necessary to ensure that the applied wheel braking torque does not cause the wheels to lock up and limit the braking torque as in the following equation (16):

$$T_{bi} \le \mu F_{zi} R \tag{16}$$

In the above equation: T_{bi} is the braking torque applied to the wheel.

The brake force distribution layer receives additional yaw torque information from the tracking layer and determines the value of brake torque applied to each wheel, ignoring rolling resistance, as shown in equation (17) below:

$$T_{bi} = \frac{\Delta M}{d_1} R \tag{17}$$

According to the control wheel selection rules and each wheel's braking torque calculation method, we can determine the wheels to be controlled in the process of anti-roll control and the control wheel's required braking torque magnitude. The actual braking torque applied is determined by the hydraulic controller. The actual braking torque is determined by the hydraulic controller as in the following equation (18):

$$T_{bi}^{*} = T_{bi} \times G_h(s) \tag{18}$$

In the above formula: T_{bi}^{*} is the braking torque after the hydraulic system.

4.Research on the Coordinated Control Strategy of Drive Anti-slip Rotation System and Transverse Pendulum Stability System

In order to improve the performance of the whole vehicle, various sub-systems such as drive anti-skidding system, traverse stability system, etc. have been developed, and in the study of each sub-system, only the impact of the individual system on the vehicle will be considered, without considering whether there will be mutual impacts and conflicts with other sub-systems. To make full use of subsystems to improve overall vehicle performance, but also to ensure that the subsystems do not conflict with each other, integrated subsystem control has gradually become a hotspot for research. Compared with each subsystem working alone, integrated control has several advantages: The subsystems can work simultaneously without negatively affecting each other to improve the performance of the whole vehicle. When applied in real vehicles, the number of sensors can be reduced, and the signals between subsystems can be shared to save manufacturing costs.

4.1. Coordinated Control Analysis

The way of integrated control has been classified into two types: integrated control and coordinated control. Integrated control combines the information collected from each controller with the control requirements of the control system, designs a central controller, and replaces the work of the sub-controllers with the designed master controller. In this way, the system can be redesigned, the decoupling between the different parts can be simplified, and the individual parts can be made more independent from each other. This does not mean simplifying individual systems, only simplifying individual systems in terms of control of time and control strength of system constraints.

4.2. Coordinated Control Targeting

The drive anti-slip control system monitors the slip rate in real time during the driving process and ensures good dynamics and longitudinal stability by adjusting the torque of the front and rear motors. The Electronic Stability Program (ESP) is a system that uses the vehicle's steering characteristics to select the most appropriate hydraulic differential braking to apply braking force to the wheels, generating a swinging torque to correct the vehicle's instability phenomenon. At high speeds, vehicles are more

susceptible to lateral instability, but with Electronic Stability Control, the hydraulic differential braking method will cause speed fluctuations and deceleration during the driving process. In other words, the intervention of the electronic stability control system will have a certain effect on the vehicle's dynamic performance. Therefore, when designing the coordinated control strategy, it is necessary to weigh the dynamics and stability of the vehicle during the driving process.

4.3. Coordinated Control Strategy Design

The threshold conditions for high and low speeds are set at 10 meters per second (36 kilometers per hour), taking into account the stability and dynamic requirements for both high and low speeds. When the vehicle speed is below 10 meters per second, the main consideration is the vehicle dynamic performance requirement; when the vehicle speed is above 10 meters per second, the main consideration is the pendulum stability requirement. The control strategy adopted is shown in Figure 6.

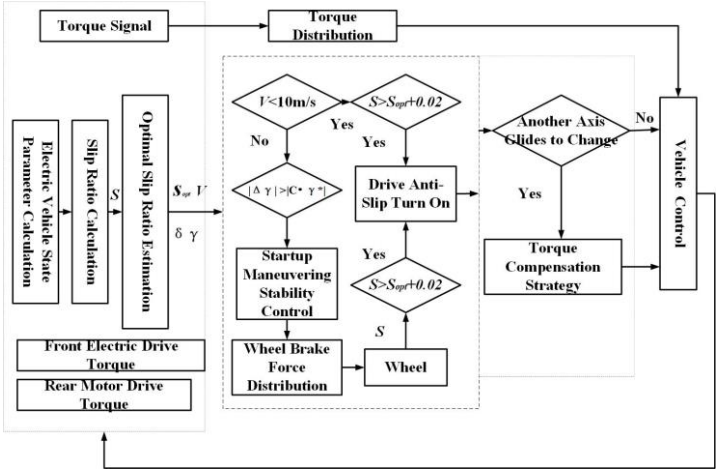

Figure 6. Coordinated control strategy logic.

The controller collects vehicle information to judge the current vehicle speed, when the judged vehicle speed is less than. When the judged speed is less than 10m/s, the main consideration is the dynamic performance of the vehicle, and the value of slip rate is used to judge whether to start the drive anti-skid control. After comparing the slip rates of the four wheels, the wheel with the highest slip rate is selected for control according to the "highest selection" rule. This ensures the best torque distribution, full utilization of the road grip, and good working condition of the vehicle. If the vehicle speed is judged to exceed 10 meters per second, activate the anti-skid control according to the slip angular velocity deviation. When the vehicle speed is judged to be more than 10m/s, it judges whether to activate the anti-skid control system according to the deviation of the lateral angular velocity.

After starting, the wheels with the most braking power are selected by analyzing the vehicle's steering information and using the hydraulic differential braking method. And the Traction Slip Control system monitors the wheels to prevent the vehicle from becoming longitudinally unstable due to excessive wheel slip.

When the traction slip control is activated, it is also necessary to apply torque compensation control to the single-axle engine that is not controlled by traction slip. Finally, the engine torque is distributed to the front and rear axles.

4.4. Coordinated Control Strategy Validation

To further validate the rationality of the coordination control strategy, the vehicle starts accelerating from an initial speed of 18 km/h with a sinusoidal steering angle applied continuously to the wheels, as shown in Figure 7. The condition is that the left side of the road has a coefficient of friction of 0.2 and the right side has a coefficient of friction of 0.6.

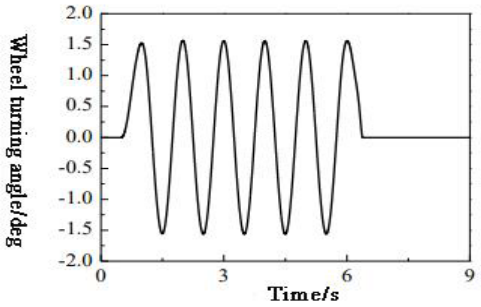

Figure 7. Continuous sinusoidal wheel angle.

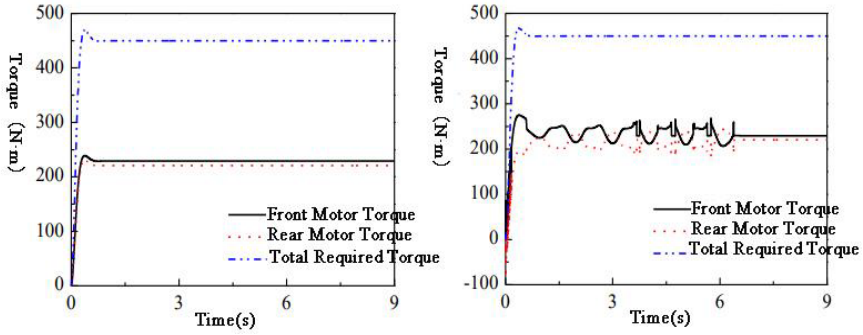

(a) Motor torque distribution before control (b) Motor torque distribution before control

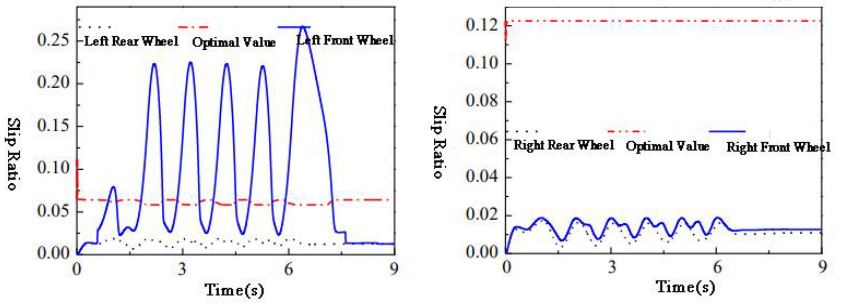

(c) Control of front left wheel slip rate (d) Control of front right wheel slip rate

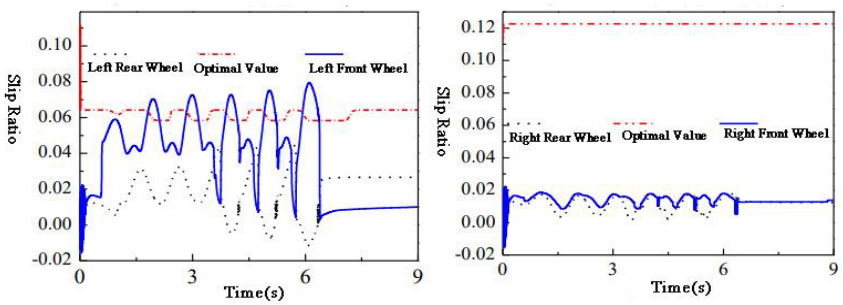

(e) Control of rear left-hand wheel slip rate (f) Control of rear right hand wheel slip rate

Figure 8. Comparison chart of slip rate before and after control.

The simulation results are shown in Figures 8.

From Figure 8(c, d), it can be seen that due to the low adhesion coefficient on the left side of the car, the peak wheel slip rate of the left front axle reached 0.28 when turning, resulting in severe skidding. However, due to the distribution of engine torque, the slip rate of the left rear wheel was only around 0.02; the right side wheels have a high road adhesion coefficient, so the slip rate was only between 0.01-0.02, without skidding. Figure 8 (a, b) shows a comparison of before and after motor torque control, which shows that after wheel slippage is detected, adjusting the torque distribution of the front. And rear motors can reduce the peak slip rate of the left front wheel to 0.08, as shown in Figure 8 (e, f). The optimum slip rate is then around 0.065, which indicates that the slip rate has not exceeded the stable range. In addition, the torque transmission does not cause other wheels to slip. The simulation results show that the coordinated control can effectively complete the control task of the traction anti-skid system and ensure the longitudinal stability of the vehicle during driving.

5.Conclusion

This paper further discusses the anti-slip and handling stability control strategies for dual-motor four-wheel drive electric vehicles, based on domestic and international research on anti-slip control and handling stability of electric vehicles. An anti-slip control strategy has been developed to address the wheel slip problem that occurs during the driving process of dual-motor four-wheel drive electric vehicles. This control strategy adopts the "high selection principle" to determine the adaptive control of one axle motor. At the same time, the compensation control strategy monitors the wheel slip rate of the other axle to prevent wheel slip on the uncontrolled axle. The designed control strategy can achieve wheel slip freedom for dual motor electric vehicles when driving on different road surfaces and ensure vehicle performance. Wheel instability problems occur in both longitudinal and lateral directions during acceleration and steering. Considering the different requirements for performance and stability at high and low speeds, a coordinated control strategy was developed for the anti-slip system and the lateral stability system. This achieved the objective of vehicle stability during acceleration and steering. The vehicle stability control performed in this thesis mainly verified the effectiveness of the control strategy. Therefore, only the yaw rate was selected as the tracking target in the upper layer of the hierarchical control, without considering the change in the centroid lateral bias angle, and only the

brake differential braking was used in the allocation layer. Future research should consider both yaw rate and centroid side bias as tracking targets, and then use mathematical programming in the allocation layer to optimize the distribution of driving forces. This paper has considered the steady-state response of the vehicle, and the next study should consider the transient response of the vehicle during the steering process to comprehensively improve the stability of vehicle handling.

References

[1] Jankowski-Mihulowicz, P.; Pawlowicz, B.; Kolcz, M.; Weglarski, M., Identification Efficiency in RFIDtex Enabled Washing Machine. Ieee Access 2023, 11, 103814-103829.
[2] Jia, K.; Lin, S.; Du, Y.; Zou, C.; Lu, M., Research on Route Tracking Controller of Quadrotor UAV Based on Fuzzy Logic and RBF Neural Network. Ieee Access 2023, 11, 111433-111447.
[3] Jin, M.; He, Y.; Yang, S.; Liu, Y.; Yan, L.; Sun, Y., Versatile RFID-Based Sensing: Model, Algorithm, and Applications. Ieee Transactions on Mobile Computing 2023, 22 (10), 6223-6236.
[4] Khalid, N.; Iyer, A. K.; Mirzavand, R., A Battery-Less Non-Hybrid Six-Port RFID-Based Wireless Sensor Architecture for IoT Applications. Ieee Sensors Journal 2023, 23 (9), 9410-9418.
[5] Kumar, A.; Singh, K.; Shariq, M.; Lal, C.; Conti, M.; Amin, R.; Chaudhry, S. A., An efficient and reliable ultralightweight RFID authentication scheme for healthcare systems. Computer Communications 2023, 205, 147-157.
[6] Lasantha, L.; Karmakar, N. C.; Ray, B., Chipless RFID Sensors for IoT Sensing and Potential Applications in Underground Mining-A Review. Ieee Sensors Journal 2023, 23 (9), 9033-9048.
[7] Li, A.; Li, J.; Zhang, Y.; Han, D.; Li, T.; Zhang, Y., Secure UHF RFID Authentication With Smart Devices. Ieee Transactions on Wireless Communications 2023, 22 (7), 4520-4533.
[8] Li, B.; Wang, Y.; Zhao, Y.; Liu, W., Enabling Fine-Grained Residual Liquid Height Estimation with Passive RFID Tags. Ieee Sensors Journal 2023, 23 (17), 20159-20168.
[9] Li, H.; Bai, J.; Wu, F.; Zou, H., A novel two-dimensional PID controller design using two-dimensional model predictive iterative learning control optimization for batch processes. Canadian Journal of Chemical Engineering 2023, 101 (12), 6959-6976.
[10] Li, J.; Wang, J., Reinforcement learning based proportional-integral-derivative controllers design for consensus of multi-agent systems. Isa Transactions 2023, 132, 377-386.
[11] Li, T.; Liu, Y.; Ning, J., SDRLAP: A secure lightweight RFID mutual authentication protocol based on PUF with strong desynchronization resistance. Peer-to-Peer Networking and Applications 2023, 16 (4), 1652-1667.
[12] Li, Y.; Bi, J.; Han, W.; Tan, W., Tuning of PID/PIDD2 controllers for integrating processes with robustness specification. Isa Transactions 2023, 140, 224-236.
[13] Li, Y.; Ma, D., Robust sampled-data PID controller design for regulation control of nonlinear systems with output delay. International Journal of Robust and Nonlinear Control 2023, 33 (11), 6371-6391.
[14] Liu, J.; Wei, T.; Chen, N.; Wu, J.; Xiao, P., Fuzzy Logic PID Controller with Both Coefficient and Error Modifications for Digitally-Controlled DC-DC Switching Converters. Journal of Electrical Engineering & Technology 2023, 18 (4), 2859-2870.
[15] Lopez-Iturri, P.; Ruiz-Feliu, R.; Picallo Guembe, I.; Klaina, H.; Tirapu Frances, F. J.; Martinez, P.; Nuin Amado, I.; Basarte, E.; Morentin, J.; Garacochea Saenz, A.; Santesteban, S.; Bravo, J.; Oteiza Echeverria, J. I.; Falcone, F., Implementation of a Low-Cost Chipless RFID System With Paper-Based Substrates Printed Tags for Traceability Applications in the Packaging Sector. Ieee Sensors Journal 2023, 23 (13), 14923-14937.